ELSEVIER

Polymer 42 (2001) 2969–2983

polymer

www.elsevier.nl/locate/polymer

Association properties of poly(ethylene oxide) modified by pendant aliphatic groups

F. Liu[a], Y. Frere[b], J. Francois[c,*]

[a]*Institute of Porous Flow and Fluid Mechanics CNPC-CAS, P.O. Box 44, Langfang, Hebei 065007, People's Republic of China*
[b]*Institut Charles Sadron, CNRS-ULP, 6, Rue Boussingault, 67083 Strasbourg cedex, France*
[c]*Laboratoire de Physico-Chimie des Polymères, CNRS-UPPA, UMR 5067, Hélioparc, 2, Avenue du Président Angot, 64053 Pau, France*

Received 28 March 2000; received in revised form 3 April 2000; accepted 12 June 2000

Abstract

Series of copolymers ethylene oxide and alkylglycidyl ether (EO-*co*-AGE), ethylene oxide-3,3-di(alkoxymethyl)propyl glycidyl ether (EO-*co*-DAGE) and poly(alkyl glycidyl ether) ((POM/POE)–PAGE) have been synthesised, as associating water-soluble polymers, where the hydrophobic substituents (less than 1% mole fraction) are, respectively, randomly distributed along the chain or present as dimers or as long sequences. The synthesis of initial hydrophobic monomers and the copolymer preparation are shortly described. The associative properties of these new associating samples were studied as functions of length, distribution, mole fraction of hydrophobes and polymer concentration, using fluorescence, light scattering and viscosimetry. Generally, these comb-like associating polymers do not exhibit thickening properties as good as those of the equivalent telechelic polymers of the same chemical composition. This difference is attributed to the formation of intra-molecular hydrophobic association favoured in cases of comb structure with respect to the telechelic ones. However, a great influence of the sequentiality of the hydrophobe distribution was observed. © 2001 Published by Elsevier Science Ltd.

Keywords: Copolymers; Aliphatic groups; Association properties

1. Introduction

The term "water-soluble associating polymer" is given to a polymer constituted by a hydrophilic skeleton that bears some hydrophobic groups either randomly distributed along the chain (grafted or comb-like) or fixed at one or two extremities (telechelic) [1]. The skeleton of branched associating polymers is most frequently polyacrylamide (PAM) [2–7], polyacrylic acid [8,9] or acrylamide–acrylic acid copolymers [10,11]. Telechelic polymers are more usually based on poly(ethylene oxide) (PEO) [12–18]. Hydrophobic groups can be either aliphatic (with a number of carbons ranging between 8 and 20), aromatic or fluorinated. Many works have been devoted to such polymers because of their attractive properties. In particular, it is well known that aqueous solutions exhibit shear thickening and shear thinning behaviours owing to the fact that hydrophobic groups gather in nano-domains, which act as temporary cross-links. Different techniques have been used to elucidate the association mechanism and relate the solution structure and rheological properties (fluorescence [17–19], light [20–23], X-rays and neutron scattering [15,16], NMR [24,25]).

Very often, rigorous interpretation is made difficult by the sample polydispersity and by a bad control of its chemistry. For example, it is known that the distribution of the hydrophobic groups along the chain plays an important role, a sequential distribution leading to a higher viscosity of the aqueous solutions than a random one [26]. However, owing to the very low amount of hydrophobes, sequentiality cannot be directly evaluated by NMR, but only deduced from kinetics arguments.

On the contrary, telechelic polymers, prepared from PEO, constitute the best models for fundamental studies, since they have a very low polydispersity and the degree of functionalisation of the extremities can be perfectly controlled [27–29]. Besides, methods of characterisation have been developed for such polymers [29]. Thus, a good picture emerges from many physico-chemical and rheological investigations, as schematised in Fig. 1. At a given critical concentration, CAC (critical association concentration), ω or α,ω-functionalised PEO associate in micelles or "flower-like" aggregates, respectively. Recent light scattering studies show that this first association step can be considered as a "closed association", which means that it is rather

* Corresponding author.

0032-3861/01/$ - see front matter © 2001 Published by Elsevier Science Ltd.
PII: S0032-3861(00)00530-9

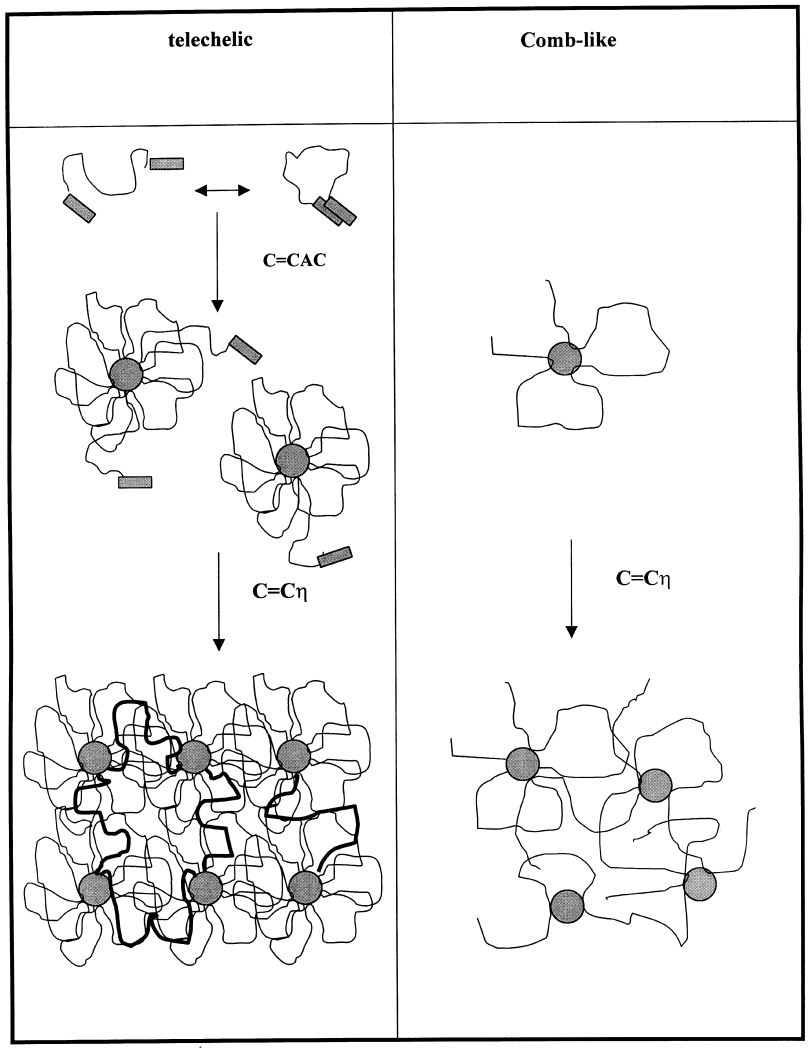

Fig. 1. Schematic representation of the association of telechelic and comb-like associating PEO in water.

co-operative. In the second step, above a second critical concentration, C_f^*, which corresponds to the overlap of micelles or "flowers", viscosity diverges from that of unmodified PEO [22,23]. Very soon, for CAC $< C < C_f^*$, a liquid order appears in the solutions as revealed by a small angle peak, in X-rays or neutron scattering curves [15,16]. For the more-associated systems, molecular weight of PEO below 6000, several narrow peaks (up to seven) indicate that the structure is cubic and for the less-associated ones, the broad peak corresponds to a degeneration of such structure. It has been shown that the elastic modulus at the plateau and the viscosity enhancing is related to a reinforcement of the organisation [29].

Whatever the systems are, branched or telechelic, the dependencies of rheological properties on number, length and chemical nature of hydrophobic groups is empirically well known. However, there are very few works dealing with the advantages and disadvantages of the one type of architecture (branched or telechelic) with respect to the other. This is due to the chemical problems encountered in preparing the two types of architecture with exactly the same chemical composition. An attempt was made to prepare telechelic associating polymers from PAM [28], but the samples were polydisperse and it was not possible to obtain directly difunctionalised samples alone; then, a separation step became necessary.

PEO seems to be a better candidate to make such a systematic comparison between branched and telechelic architecture. In this work, we present the synthesis of hydrophobic PEO with pendant aliphatic chains. We have focused our attention on the problem of the hydrophobe distribution. For this purpose, copolymerisations of ethylene oxide with comonomers or macromonomers having one or more aliphatic groups were performed (as schematised in Fig. 2). The association was studied by fluorescence, light scattering, neutron scattering and viscosimetry. The phase diagrams of these copolymers were also established. The results were systematically compared with those previously obtained with telechelic PEO.

Name	Chemical formula	Schema	Parameters
(ethylene oxide-alkylglycidyl ether)copolymers (EO-AGE)co	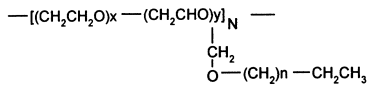	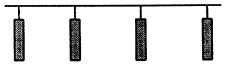	n =6,10,14, 20 $3.10^{-3} < Y < 8.10^{-3}$ $1000 < N < 2000$
(ethylene oxide-3,3-(dialkoxymethyl)propyl glycidyl ether)copolymers (EO/DAGE)co	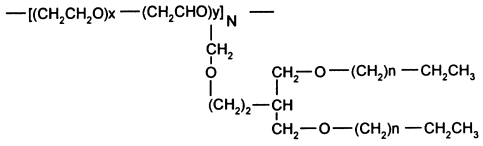	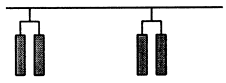	n = 6, 10, 14 $1{,}5.10^{-3} < Y < 3{,}2.10^{-3}$ N = 2000
poly(methyleneoxide-alt (PEO)polyalkylglycidyl ether) (MO/PEO-PAGE)co	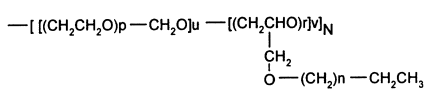	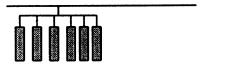	$y = \frac{vr}{vp + vr}$ n = 8, r = 20 n = 10, r = 24 $2.10^{-3} < y < 8.10^{-3}$

Fig. 2. Name, chemical formula and schematic structural representation of the different samples studied in this work.

2. Experimental

2.1. Copolymer synthesis methods

(i) *Ethylene oxide–alkyl glycidyl ether copolymers (EO-co-AGE).* In a first step, alkyl glycidyl ethers (AGE) were obtained by reaction of epichlorydrine (EC) with the corresponding alcohol, in the presence of sodium hydroxide and trimethylammonium hydrogenosulphate ($(But)_4NHSO_4$), as described in Ref. [30]. Reaction 1:

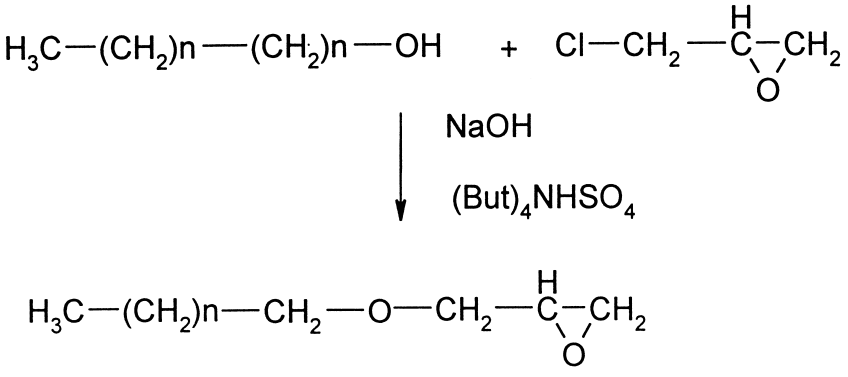

Copolymerisations of EO and AGE were performed with several catalysts of the type described by Vandenberg [31,32], in various solvents, as reported in Table 1.

(ii) *Ethylene oxide-3,3-di(alkoxymethyl) propyl glycidyl ether copolymers (EO-co-DAGE).* Several methods were tested for substituted ethylene oxide: 3,3-di(alkoxymethyl) propyl glycidyl ether (DAGE) synthesis, but the reaction yield was too low. The method we have used requires nine steps. The four first steps allow us to obtain the 2-benzyl-oxyethanol mesylate. The next five steps finally lead us to obtain the DAGE. Fig. 3 gives the reaction scheme of this synthesis. Copolymerisations of ED with DAGE were only performed with catalyst II in toluene.

(iii) *Poly(methylene oxide-alt-(PEO)); poly(alkyl glycidyl ether) ((POM/POE)-PAGE).* The first step is the polymerisation of AGE, which was performed according to the method of Vandenberg [31,32]. The second step is the coupling of PAGE, which is based on a Williamson reaction in dichloromethane. All the details of the reactions are given elsewhere.

Table 1
Nomenclature, conditions of synthesis and characteristics of copolymers (EO-*co*-AGE) and (EO-*co*-DAGE): catalyst I, (Et_3Al–$0.5H_2O$–0.5AcAc); catalyst II, (iso-Bu_3Al–$0.5H_20$) (τ, grafting ratio; $\bar{M}_w$, weight average molecular weight)

Polymer and n	Synthesis conditions					Characteristics		Nomenclature
	Catalyst	Solvent	% Catalyst	Temperature (°C)	Yield (%)	τ (%)	$\bar{M}_w$	
(EO-*co*-AGE)								
$n = 8$	II	Heptane	4	35	32	0.3	5×10^4	M-08-30-50 (1)
	II	**Heptane**	4	35	18	0.62	5×10^4	M-08-62-50 (2)
	I	Ether	4.5	30	79.7	0.64	10^5	M-08-64-100 (3)
	II	Heptane	4	35	18	1.02	5×10^4	M-08-102-50 (4)
$n = 12$	II	Heptane	3.9	35	36	0.32	5×10^4	M-12-32-50
	II	Heptane	4.6	90	22	0.36	5×10^4	M-12-36-50
	II	Heptane	6.3	35	40	0.45	5×10^4	M-12-45-50
	I	Ether	6.5	30	61.6	0.60	10^5	M-12-60-100
$n = 16$	II	Heptane	6.5	35	51	0.23	5×10^4	M-16-23-50
	II	Heptane	4.0	35	14	0.25	5×10^4	M-16-25-50
	II	Heptane	4.6	90	34	0.46	5×10^4	M-16-46-50
	I	Ether	5.6	30	72.5	0.74	10^5	M-16-74-100
$n = 22$	I	Ether	5.0	30	42.4	0.21	10^5	M-22-21-100
	II	Heptane	4.6	90	34	0.30	5×10^4	M-22-30-50
	I	Ether	6.0	30	54.9	0.33	10^5	M-22-33-100
	I	Ether	4.5	30	60.9	0.94	10^5	M-22-94-100
(EO-*co*-DAGE)								
$n = 8$	I	Toluene	5.3	30	59.7	0.4	10^5	D-08-40-100
	I	Toluene	5.3	30	29.8	0.94	10^5	D-08-94-100
$n = 12$	I	Toluene	5.3	30	52.8	0.34	10^5	D-12-34-100
	I	Toluene	5.3	30	35.4	0.68	10^5	D-12-68-100
$n = 16$	I	Toluene	5.3	30	78.4	0.3	10^5	D-16-30-100

2.2. Polymer characterisation

Polymer samples were characterised by ^{1}H NMR, using a spectrometer Brucker AC-200 (200 MHz). Hexamethylcyclotrisiloxane ($((CH_3)_2$–$SiO)_3(D_3)$) was used as reference, to improve measurement accuracy. A solution 7.1×10^{-7} mol ml^{-1} of D_3 was prepared in carbon tetrachloride (CCl_4) and copolymers (approximately 20.4 mg) were dissolved in 2 ml of this solution. Spectra were registered with an external reference (heavy water contained in a thin capillary introduced in the NMR tube). Fig. 4 shows an example of the spectrum obtained with the copolymer M-16-34-50: the main peak, between 3.5 and 3.8 ppm refers to CH_2 of PEO chain. The grafting ratio τ (or mole fraction of pendant groups in the chain) was obtained by the following relation

$$\tau = \frac{A_C C_{D_3} n_{D_3} M_{EO}}{2 A_D n C_p} \quad (1)$$

where A_C and A_D are, respectively, the peak area of the pendant group (1.4 ppm) and reference methylene (0.26 ppm), $2 \times n$ and $n_{D_3} = 18$ are the number of protons in pendant groups and reference, C_{D3} is the molar concentration of D_3 and C_p, the polymer concentration in mg l^{-1}. M_{EO} is the molecular weight of the EO unit. This approximate relation takes into account the fact that τ is generally very low.

2.3. Physico-chemical methods

(i) *Turbidimetry.* Solubility diagrams of our polymers were obtained by turbidimetry, using a Mettler FP80-81 apparatus. The solutions were put in capillaries inside an oven subjected to an increase of temperature. Clouding points correspond to the temperature for which the intensity of light scattered at 90° suddenly increases.
(ii) *Light scattering.* Static light-scattering measurements were performed with a SEMATECH photogonio-diffusometer, equipped with a laser source He–Ne (wave length: 632 nm), inside a scattering-angle range from 30 to 150°. We used a home-built dynamic light-scattering apparatus (M. Duval). The wave length of the ionised argon laser (Spectra Physics 2020) is 488 nm. It works with a Hamatsu photo multiplier. The auto-correlation function is obtained using an ALV 3000 correlator of 194 channels and analysed with the CONTIN method.
(iii) *Fluorescence.* Fluorescence spectra of pyrene in polymer solutions were recorded with a spectrofluorometer Hitachi F 4010. Pyrene was used at its saturation

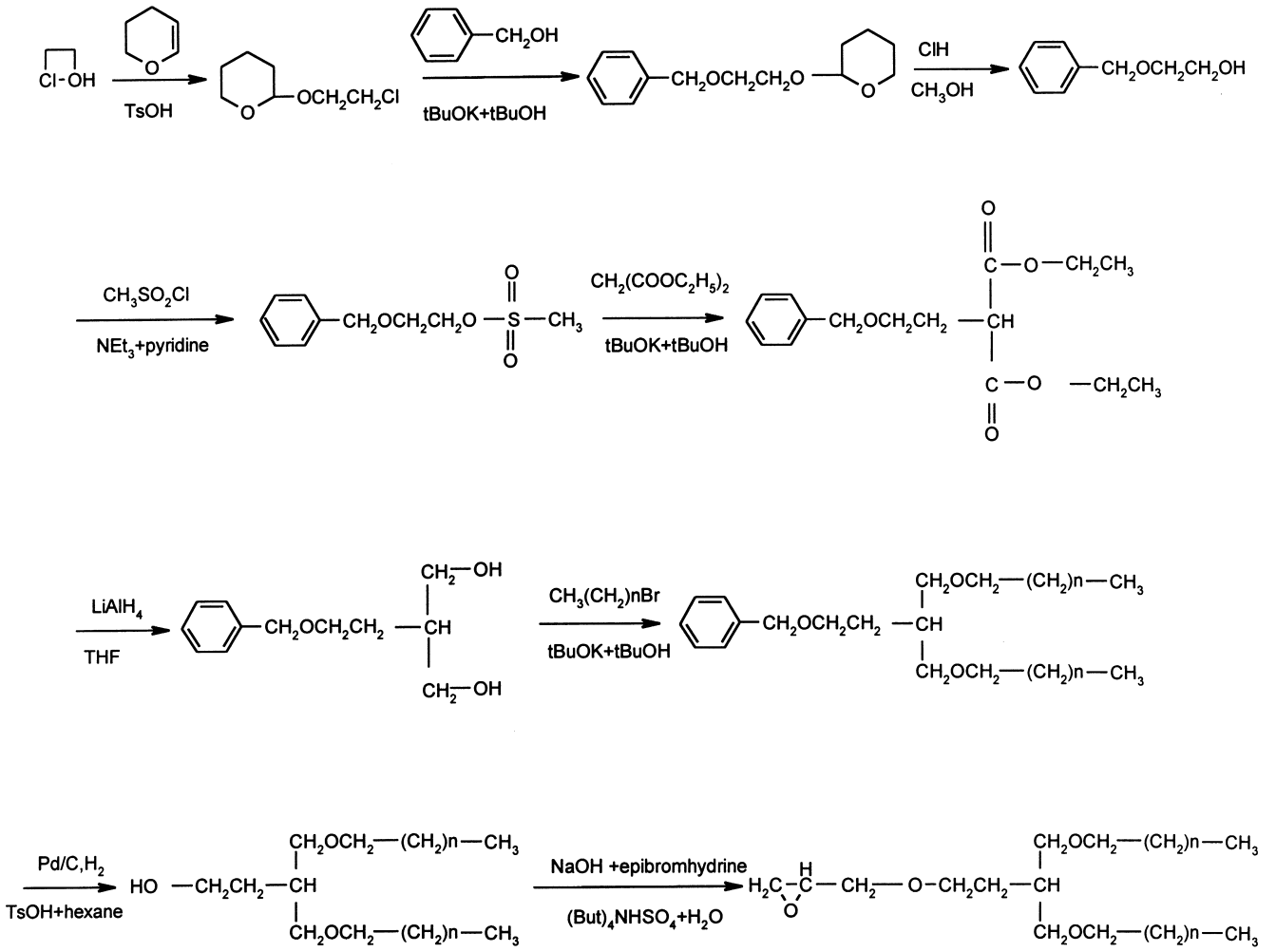

Fig. 3. Chemical reaction scheme for the preparation of DAGE.

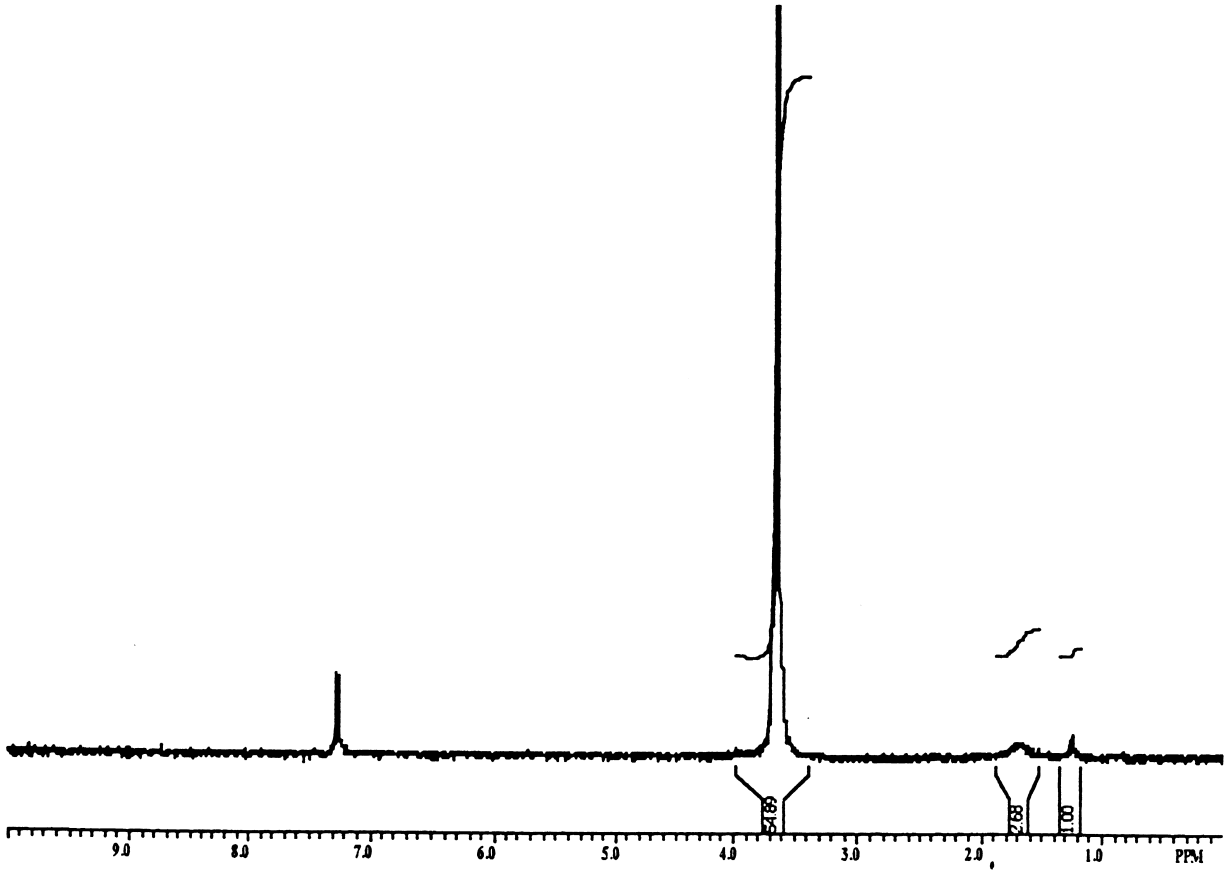

Fig. 4. Example of ^{1}H NMR spectrum (obtained with sample M-16-34-50).

concentration in water (5×10^{-5} M). The excitation wave length was set to 335 nm and emission measurements were performed between 350 and 550 nm. The ratio of the first to the third emission peak intensities is expected to abruptly drop when micellisation occurs as well-demonstrated by numerous works [33,34]. The cell was thermostated at 25 ± 0.1°C.

(iv) *Viscosimetry and rheology.* Two different viscometers were used according to viscosity range:

- For lower polymer concentrations, when viscosity is Newtonian and close to that of water, an automatic capillary viscometer "Viscologic Ti.1" from SEMA-TECH was used. It is equipped with a glass device of the Ubbelohde type (capillary of 0.4 mm ∅). The apparatus was thermostated at 25 ± 0.1°C.
- For higher polymer concentrations, for which solutions are no more Newtonian, a low-shear viscometer "Low shear-Contraves 30", with couette cells 1–1 or 2–2 according to the viscosity value was used. Temperature was kept constant at 25 ± 0.1°C.

Table 2
Characteristics of block copolymers

Sample	n	Grafting ratio τ	Weight average molecular weight
B-08-40-160	8	0.4	167 000
B-08-80-170	8	0.8	170 000

3. Results

Tables 1 and 2 give information about sample synthesis and characteristics: molar fraction of pendant chains τ and weight average molecular weight. Sample nomenclature is defined by one letter M, D or B for (EO-*co*-AGE), (EO-*co*-DAGE) and (MO/PEO-*co*-PAGE), respectively. The first number is the total number of carbons in pendant aliphatic chains n': if the precursor alcohol has six carbons, $n' = 8$. The second number is $\tau \times 100$. The third one is the weight average molecular weight $\bar{M}_w$ divided by 1000. Let us note that it is very difficult to measure $\bar{M}_w$ with a good accuracy. Several solvents were used, where association was not expected. However, if the solvent is too polar, hydrophobic groups associate while a solvent that is not polar enough does not allow PEO to be solubilised. The solubility parameter of PEO is $\delta = 9.9$ (cal cm^{-3})$^{1/2}$ and among several solvents investigated: H_2O, methanol, acetonitrile, tetrahydrofuran (THF), chloroform $CHCl_3$, toluene and heptane

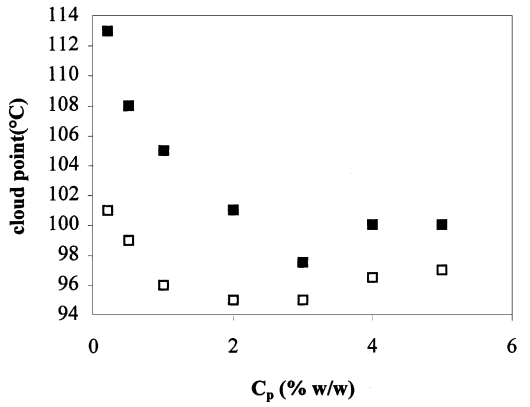

Fig. 5. Cloud points of aqueous solutions of samples M-12-45-60 (□) and M-12-36-60 (■) as a function of concentration.

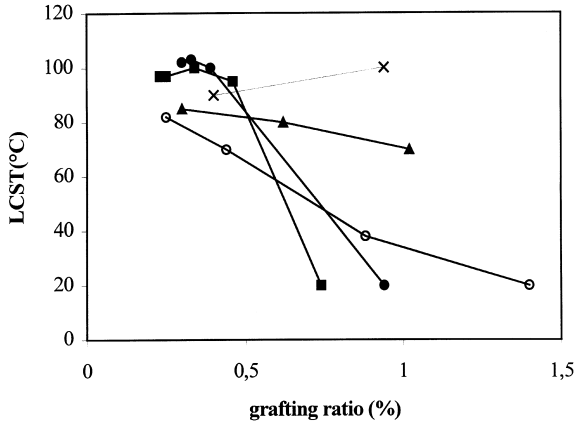

Fig. 6. LCST values as a function of the parameter τ, for different species of associating polymers: series M-16 (■); series M-22 (●); series M-08 (▲); series D-08 (×); and telechelic polymers (○).

of $\delta = 23.4$, 14.5, 11.9, 9.1, 9.3, 8.9 and 7.4 (cal cm^{-3})$^{1/2}$, THF and $CHCl_3$ should be the best. However, even in these two cases, light-scattering measurements reveal the presence of a small fraction of aggregates. Nevertheless, by neglecting the excess of scattered intensity at small angles, we have found that samples prepared by using catalyst I were close to 10^5 while those prepared with catalyst II had a molecular weight of around 5×10^4. While telechelic polymers were successfully characterised by size exclusion chromatography using the mixture H_2O/acetonitrile [29], we did not obtain good results with these comb-like polymers.

3.1. Phase diagrams

Aqueous solutions of unmodified PEO exhibit phase separation upon heating [35–38]. For infinite molecular weight, the lower critical solution temperature, LCST, is 100°C [36]. Many theories were proposed to describe such behaviour, which is quite characteristic of polar systems [36–39]. It is generally considered that H_2O molecules are strongly bound to PEO chains through hydrogen bonds with the oxygen atoms of PEO. This modifies the solvent/polymer interaction parameter, χ, which is much lower than that calculated from the solubility parameter, at least at room temperature. However, the solvent is released upon heating and phase separation occurs. The variation of LCST with the chemical composition of telechelic modified PEO was systematically investigated [16,19]. It was found that the presence of aliphatic chains with $n = 12$ and 18 does not decrease LCST with respect to that of the precursor, in the case of ω-functionalised PEO (ω-PEOM). At the opposite, a very high decrease was found for the α,ω-functionalised samples (α,ω-PEOM). This can be at least qualitatively understood from the "flower" model. Indeed, as soon as "flowers" are formed, there is a competition between attractive forces (owing to the fact that the two hydrophobes [39] of a same chain prefer to lie in different neighbouring micelles rather than in the same micelle) and repulsive forces between the PEO corona. The first ones can induce phase separation at a temperature which decreases upon decreasing the $\bar{M}_w$ of PEO chains (for instance, for $\bar{M}_w = 4000$ and $n = 12$, phase separation occurs down to 0°C, between a rich polymer phase (30%) and a very dilute solution. However, owing to repulsive potential between micelles, the concentrated phase is well organised in a cubic array. It is clear that, in the case of (ω-PEOM), only repulsion plays a role and the presence of one aliphatic chain does not lower the LCST. In such cases, with temperature between 0 and 100°C and $C_p >$ CAC, a liquid order is obtained.

As shown in Fig. 5, the variation of the cloud point versus concentration is similar to that observed for the PEO precursor, with a critical concentration (concentration at the minimum of curve) of about 2%. LCST values measured with our copolymers are compared with those obtained for α,ω-PEO [16,29], in Fig. 6. The parameter used to make this comparison is τ, which has the same meaning for both types of polymers and is calculated as

$$\tau = \frac{2M_{EO}}{\bar{M}_N} \quad (2)$$

where $\bar{M}_N$ is the number average molecular weight.

For the lower values of τ, approximately <0.6%, an increase of τ has no influence on the solubility while, surprisingly, an increase of n, at constant τ, results in a slight increase of LCST. Indeed, a lowering of LCST (with respect to that of the parent PEO = 100°C) is observed for $n = 8$ but not when $n = 16$ or 22.

Further, LCST depression is higher for (EO-*co*-DAGE) than for (EO-*co*-AGE), ($n = 8$). In the same range of τ, LCST of ω-PEOM with $n = 12$ is lower than those of all the comb-like copolymers with $8 < n < 22$. Moreover, for $\tau = 0.44\%$ and $\bar{M}_w = 20\,000$, α,ω-PEOM with aliphatic chains of 18 carbons phase separate at room temperature. These results for copolymers are surprising since LCST does not vary as expected by considering simply the hydrophobic–hydrophilic balance. Besides, they show that the

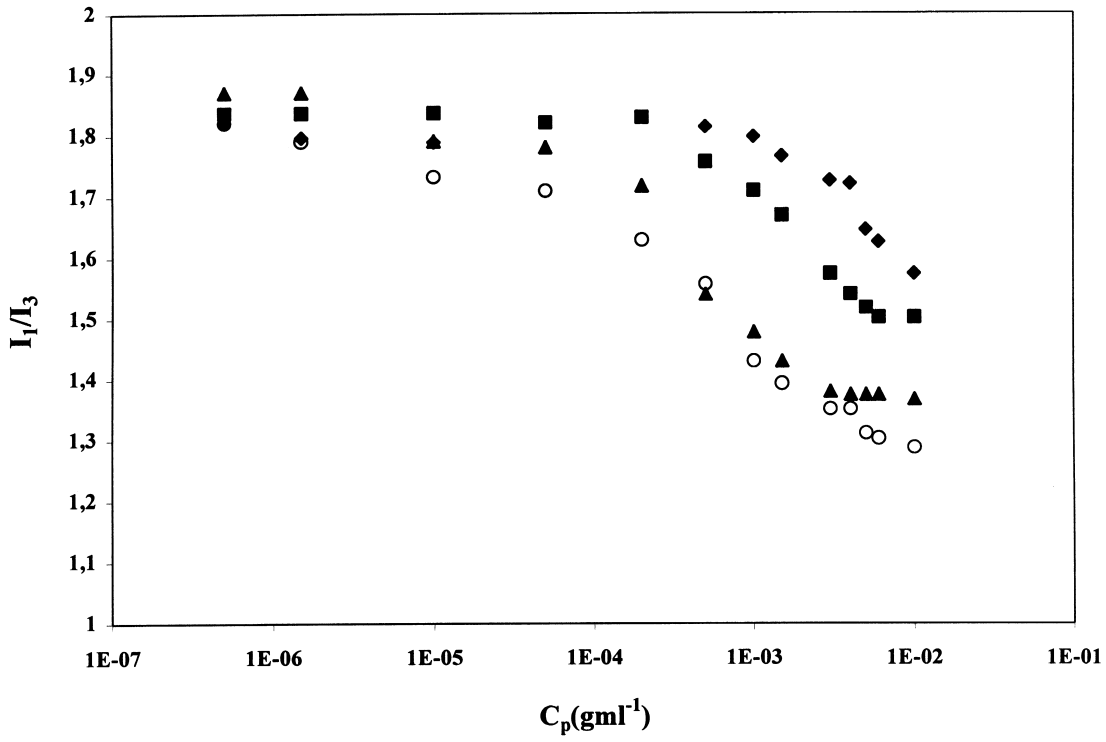

Fig. 7. Variation of the ratio I_1/I_3 versus polymer concentration — influence of the length of the hydrophobic groups: M-08-30-50 (◆); M-12-32-50 (■); M-16-25-50 (▲); and M-22-30-50 (○).

polymer architecture has great importance, since the presence of the same fraction of hydrophobic groups in the chain induces a phase separation more easily if they are at the extremities of the chains or distributed along a longer chain.

For high values of τ, $\tau > 0.6\%$, a less-surprising behaviour is observed, in the series of (EO-*co*-AGE): the higher n and τ, the lower LCST. Nevertheless, for (EO-*co*-DAGE) with $n = 8$, no lowering of LCST appears even up to $\tau = 1\%$.

One must keep in mind that some systems behave as ω-PEOM, without loss of solubility while others exhibit a low water solubility. We will see later that the first behaviour may correspond to intra-molecular micellisation, while the second one reflects a dominance of inter-molecular micellisation. All the other experimental results give evidence for such an interpretation.

3.2. Fluorescence

In this series of experiments, we have systematically measured the ratio I_1/I_3 of the first to third emission peaks of pyrene dissolved in copolymer solutions. In Fig. 7, some examples of curves obtained for the series (EO-*co*-AGE) at approximately the same τ are reported. Variation of I_1/I_3 versus polymer concentration (C_p) undergoes a drop at a concentration which decreases when n increases, which is consistent with an enhancing of the polymer hydrophobicity. Nevertheless, the transition is broad, occurring over 4 to 2 decades, and the broadness systematically increases upon increasing n. In Table 3, are reported (a) values of "CAC" (taken as the inflexion point of curves $I_1/I_3 = f(C_p)$), (b) the number of decades, ΔN, for I_1/I_3 drops

Table 3
Fluorescence results: CAC taken as the inflexion of the curve $I_1/I_3 = f(C)$, number decade between the high and the low plateaux of I_1/I_3 and value of I_1/I_3 at the low plateau

Sample	CAC (gm l^{-1})	Number of decades ΔN	$(I_1/I_3)_p$ final plateau
M-08-30-50	4×10^{-3}	1	1.56
M-12-32-50	1×10^{-3}	1.5	1.5
M-16-25-50	6×10^{-4}	2	1.34
M-22-30-50	4×10^{-4}	3.5	1.24
M-08-62-50	2×10^{-3}	1.5	1.28
M-08-102-50	10^{-3}	2	
D-08-94-100	8×10^{-4}	2.5	1.18
B-08-40-50	8×10^{-4}	4	0.98

from the value 1.9 or 1.8, usually measured in pure water (or for surfactants solutions if $C_p <$ CMC, the critical micellar concentration) and the lower plateau at high concentration $(I_1/I_3)p$, and (c) values of I_1/I_3 at low and high concentration plateaux.

(i) CAC decreases when n and τ increase, which corresponds to simple expected results, but CAC also depends strongly on sequentiality of the hydrophobe distribution.
(ii) The broadness of the transition, ΔN, is related to the same parameters: high CAC values are associated to the sharper transitions, low CAC values to broader transitions.
(iii) $(I_1/I_3)p$ values follow the inverse evolution as those of ΔN.
(iv) As shown in Fig. 8 also, sequentiality has a very important influence since sample B-08-40-50 has a CAC value lower than that of M-08-102-50 of much higher grafting ratio. Besides, the initial value of I_1/I_3 and $(I_1/I_3)p$ are, respectively, lower and higher for the blocky sample than for M-08-102-50 and D-08-92-100.

In Fig. 9, results obtained for different polymers with aliphatic chains ($n = 12$) are compared; however, the parameter used here is no longer polymer concentration, but the molar concentration of hydrophobic groups (HG) in mol l^{-1}. Indeed, if the association mechanism or architecture were the same for all the samples independently, micellisation should occur for the same molar concentration of HG $(CAC)_{HY}$. Fig. 9 indicates that the results obtained for α,ω-PEOM and ω-PEOM are almost superimposed in such representation, which shows that only the average concentration of HG rules out the association [29]. Behaviour of (EO-*co*-AGE) copolymers strongly differs from that obtained for telechelic samples. The transition is much broader and $(CAC)_{HY}$ much lower. This indicates that architecture controls micellisation much more than HG concentration.

In conclusion, fluorescence measurements of the emission spectrum of pyrene indicate that hydrophobic nanodomains are present in copolymers solutions. Nevertheless, according to their chemical composition and architecture, transition is more or less broad. We will discuss later whether I_1/I_3 variations reflect micellisation at a given concentration or the probe distribution in water and micelles, already formed at very low concentration.

3.3. Light scattering

Not many experiments of static light scattering have been performed on comb-like associating polymers. This is due to the fact that particle molecular weight cannot be considered as constant when concentration increases. For a scattered intensity value, at a given concentration and 0 angle, there are two unknown parameters $\bar{M}_w$ and the virial term [22,23,29].

$$\frac{KC_p}{\Delta I} = \frac{1}{\bar{M}_w} + 2A_2C_p = \frac{1}{\bar{M}_{wapp}} \quad (3)$$

K is an optical constant and ΔI is the excess of scattered intensity of the solution with respect to the solvent, $\bar{M}_w$ is the molecular weight averaged on the double distribution of the unimers and aggregates:

$$\bar{M}_w = C_A \frac{\sum n_{iA}M_{iA}^2}{\sum n_{iA}M_{iA}} + (1 - C_A)\frac{\sum n_{iU}M_{iU}^2}{\sum n_{iU}M_{iU}} \quad (4)$$

where the two terms correspond to the contribution of the aggregates of concentration C_A and unimers of concentration $(1 - C_A)$, respectively.

The second virial also reflects the interactions unimers/unimers, aggregates/aggregates and aggregates/unimers. In associating systems, it is usual to find three parts in the variation of $KC_p/\Delta I = I$ versus C_p:

- for $C_p <$ CAC, I increases due to the positive virial of unimers;
- for $C_p =$ CAC, I starts to drop, since association induces an increase of $\bar{M}_w$ up to another concentration C_p^{**};
- for $C_p > C_p^{**}$, I increases again.

This behaviour has been described well for ω-PEOM and α,ω-PEOM in recent papers [23,29]. Such behaviour is interpreted in terms of a competition of the variations of the two terms of Eq. (3). Indeed, the first term decreases, while the second one increases if $A_2 > 0$. In dynamic light scattering, in the first regime, one only measures the diffusion coefficient of unimers; in the intermediate one, a second low relaxation peak appears whose area increases upon increasing C_p up to C_p^{**} for which the ratio of the areas of the fast to the slow relaxation peaks increases again. In fact, the same explanation as that used for static light scattering may be used.

We have only studied a sample of (EO-*co*-AGE), in a concentration range between 0 and 1%. We can distinguish two ranges:

(i) $C_p < 0.54\%$, by extrapolation at $C_p = 0$, one finds $\bar{M}_{wapp} = 52\,000, A_2 = 210^{-4}$ cm^3 g mole^{-1} and the average radius of gyration $\bar{R}_g = 239$ Å.
These values should correspond to the unimer alone. The average $\bar{R}_g$ is, however, higher than that calculated from the empirical law given by Denavand and Selser [41]:

$$\bar{R}_g = 0.215\bar{M}_w^{0.583} \quad (5)$$

($\bar{R}_g = 163$ Å).
In this range of concentration, two peaks are observed in the relaxation time distribution, corresponding to hydrodynamic radii of $\bar{R}_H = 98$ and 1400 Å. The value of $\bar{R}_H$ associated with the fast mode is also slightly higher than that calculated from the Denavand and Selser law [41]:

$$\bar{R}_H = 0.145\bar{M}_w^{0.571} \quad (6)$$

($\bar{R}_H = 72$ Å).
The slow mode amplitude is very low with respect to that of the fast one. Nevertheless, the existence of this mode is

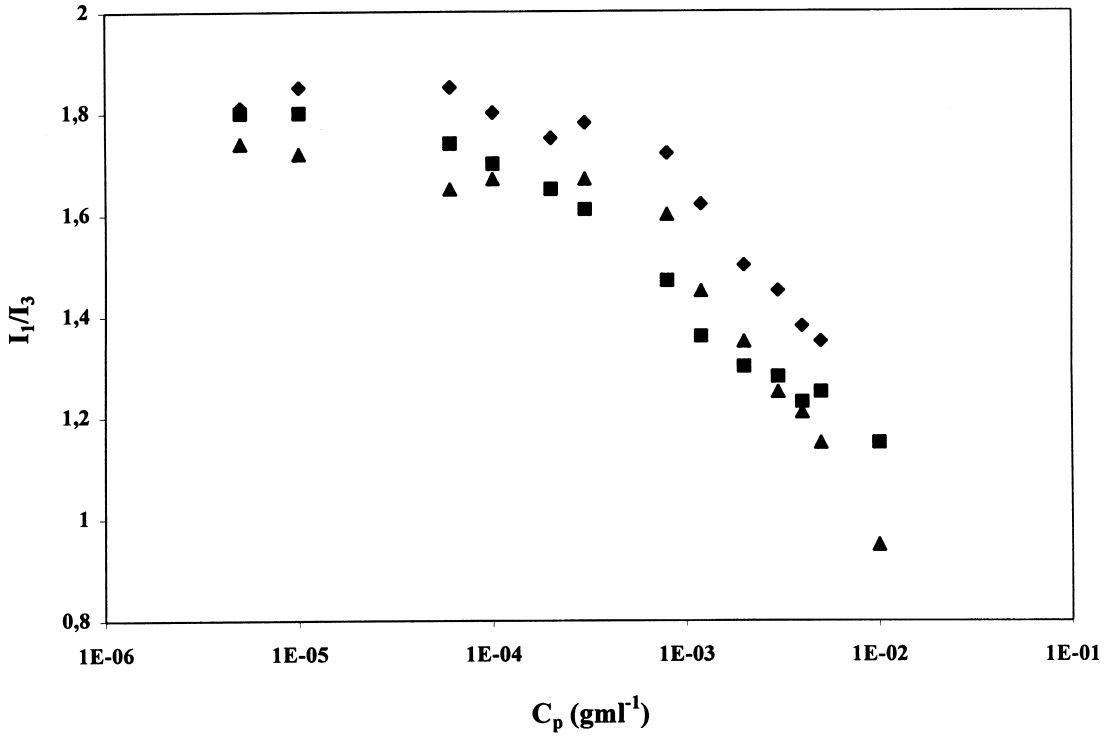

Fig. 8. Variation of the ratio I_1/I_3 versus polymer concentration — influence of the grafting sequentiality: M-08-102-50 (◆); D-08-94-100 (■); and B-08-40-50 (▲).

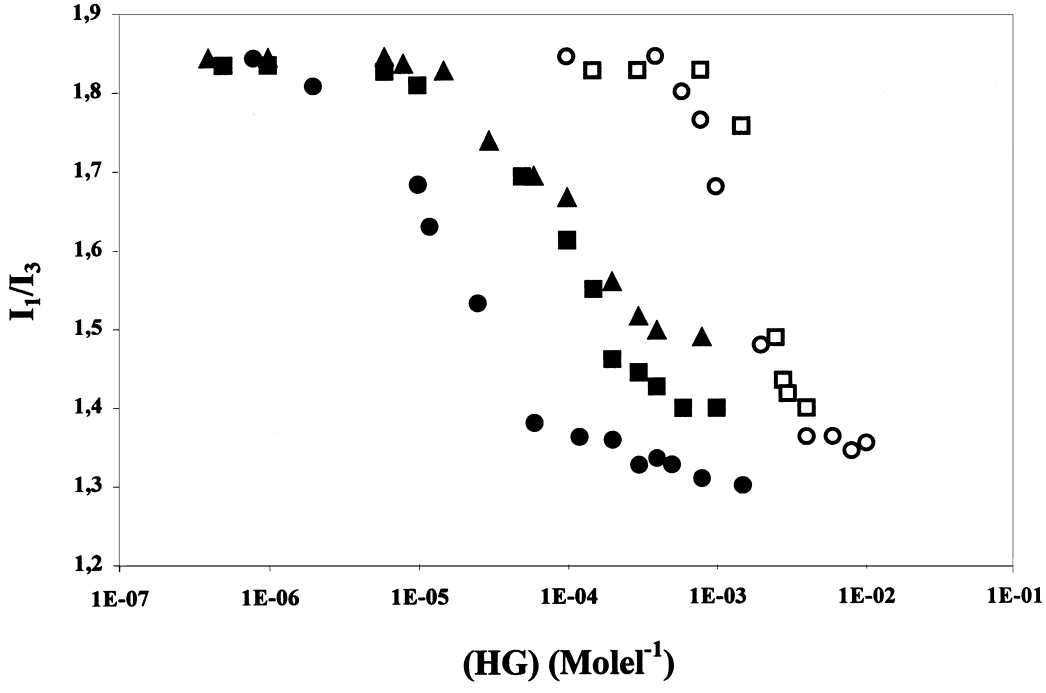

Fig. 9. Variation of the ratio I_1/I_3 as a function of the molar concentration of hydrophobes, for different species of polymers (length of hydrophobes, 12 carbons): ω-PEOM ($M = 20\,000$) (□); α,ω-PEOM ($M = 20\,000$) (○); M-12-30-50 (▲); M-12-45-50 (■); and M-12-60-100 (●).

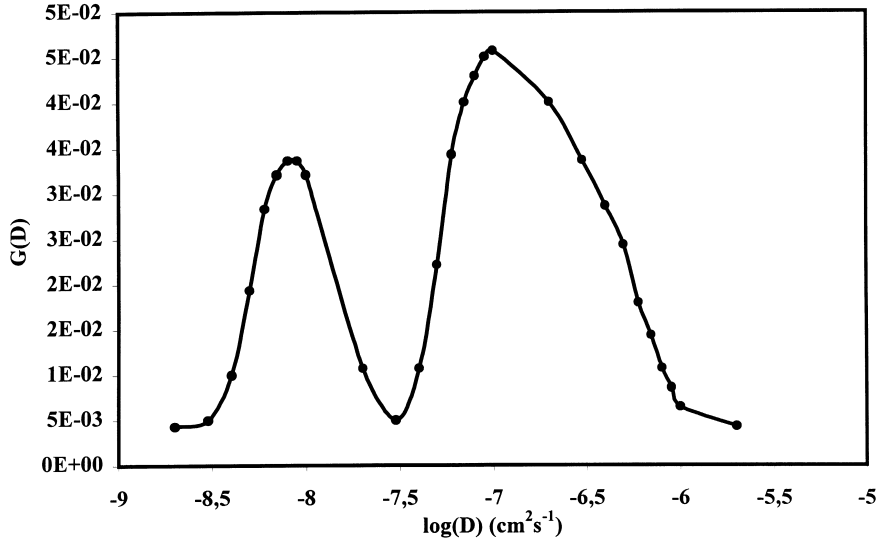

Fig. 10. Dynamic light scattering experiments on solutions of M-16-25-50 ($C = 9.9 \times 10^{-3}$ g cm^{-3}); distribution of the diffusion coefficients.

consistent with the overestimation of $\bar{R}_g$. Fluorescence has indicated formation of hydrophobic nano-domains for concentrations much lower than those investigated here.

(ii) For $0.54 < C_p < 1\%$, the average radius of gyration is slightly higher and $\bar{M}_w = 55\,000$. Fig. 10 shows that the two modes give rise to well-separated distribution peaks corresponding to apparent hydrodynamic radii of 98 and 1400 Å, respectively. Nevertheless extrapolation to $C_p = 0$ gives $\bar{M}_w = 52\,000$. This indicates that even in this range of concentration, inter-molecular association is a negligible phenomenon and that the I_1/I_3 decrease, which occurs at much lower concentration for this sample (CAC $= 6 \times 10^{-4}$ g/ml), only reflects an intra-molecular association.

By comparison, light-scattering measurements on a solution of α,ω-PEOM have shown a high increase of $\bar{M}_w$ for concentrations very close to CAC determined by fluorescence. It is quite certain that in this case, the I_1/I_3 drop indicates inter-molecular association of the hydrophobes.

3.4. Viscosity and rheology measurements

The influence of several parameters was investigated:

- *Hydrophobe length.* Fig. 11 shows that two different behaviours can be distinguished according to the concentration range. Samples M-12-32-50 and M-16-32-50, which differ only by the τ value are compared. For $C_p < 2\%$, the reduced viscosity (η_{red}) of associative copolymers is lower than that of the parent PEO of the same molecular weight and the discrepancy is higher for M-16-32-50 than for M-12-32-50. This result indicates intra-molecular association resulting in a chain collapse and a molecular dimension decrease. This was already observed for polyacrylamide-based associative polymers. For $C_p > 2\%$, divergences of η_{red} with respect to the

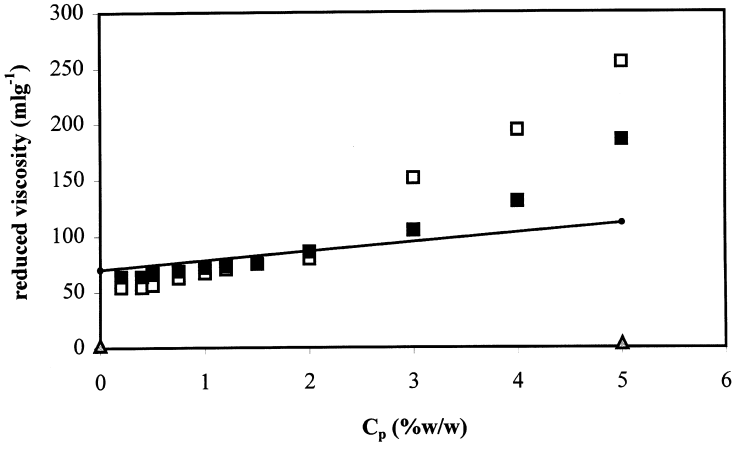

Fig. 11. Reduced viscosity of M-12-32-50 (■) and M-16-32-50 (□) versus concentration; straight line corresponds to PEO of molecular weight 5×10^4.

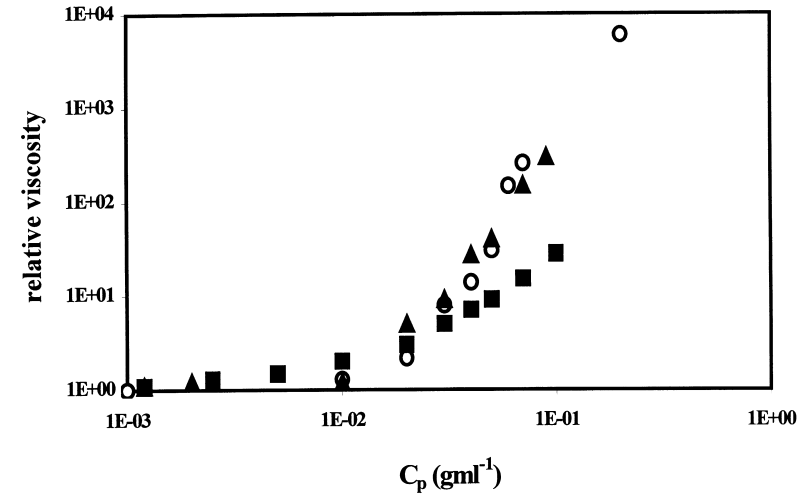

(a)

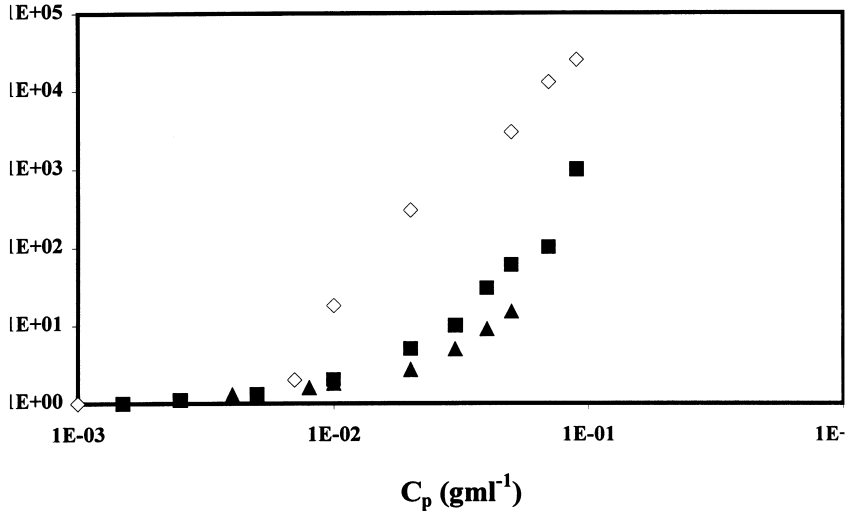

(b)

Fig. 12. Relative viscosity versus concentration. (a) M-12-32-50 (□); M-12-60-100 (■); and α,ω-PEOM ($M = 20\,000$, 12 carbons) (○). (b) M-16-32-50 (▲); M-12-74-100 (■); and α,ω-PEOM ($M = 20\,000$, 16 carbons) (✧).

reference curve (pure PEO) are observed for both M-12-32-50 and M-16-32-50, but the discrepancies are higher in the second case.

For M-08-30-50, the variation of $\eta_{red} = f(C_p)$ is almost superimposed with that of the parent polymer. Increase of the hydrophobe length enhances both intra- and intermolecular association, inducing at low and high concentration, a loss or an increase of viscosity, respectively.

Let us note that for sample M-16-25-50, close to sample M-16-32-50, no significant increase of molecular weight was measured by light scattering up to $C_p = 1\%$, which is consistent with the fact that reduced viscosity of M-16-32-50 diverges only for $C_p > 2\%$. In Table 4, we have gathered several viscosity results, which show that the hydrophobe length effect is the same for a higher grafting ratio (around 0.70%).

- *Grafting ratio.* this parameter is obviously very important for the viscosimetric behaviour. Its increase enhances η_{red}, at least up to the ratio where the samples become no more soluble in water. For instance, solutions of M-22-33-100 are liquids of high viscosity while those of M-22-94-100 appear as "gels" within the same concentration range. (The term of "gels" for such systems is inappropriate, since a flowing zone is always observed in the rheological measurements. It simply means that the flowing time of the systems is very long but not infinite). Unfortunately, we did not have enough samples of the same molecular weight and same hydrophobe length to

Table 4
Comparison of the different critical concentrations: critical overlap concentration of the parent polymer C^*, CAC given by fluorescence and C_η where viscosity diverges and viscosity results at 5 and 10%

Sample	C^* (gm l^{-1})	CAC (gm l^{-1}) fluorescence	C_η (%)	η_{red} (5%) ml g^{-1}	η_{red} (10%) ml g^{-1}
M-08-30-50	1.45×10^{-2}	4×10^{-3}	–	60	–
M-08-64-100	9×10^{-3}	–	–	200	350
M-12-32-50	1.45×10^{-2}	1.5×10^{-3}	3	180	–
M-12-60-100	9×10^{-3}	–	3	800	2700
M-16-26-50	1.45×10^{-2}	6×10^{-4}	2.5	–	–
M-16-32-50	1.45×10^{-2}			250	
M-16-74-100	9×10^{-3}	− 2	–	1200	9500
M-22-33-100	9×10^{-3}	4×10^{-4}	–	100	200
D-08-40-100	9×10^{-3}	–	4	450	1200
D-08-94-100	9×10^{-3}	1×10^{-3}	3	120	5000
B-08-40-160	–	–	–	400	–
B-08-80-170	–	–	–	40 000	–

perform an exhaustive study of the influence of the grafting ratio. Nevertheless, it is interesting to observe that samples M-12-6-100 and M-16-74-100 have much higher η_{red} than M-22-30-100. Moreover, the influence of the average grafting ratio τ is clearly seen in Fig. 12a and b.

- *Polymer architecture.* In Fig. 12a, we compare grafted sample M-12-32-50 and M-12-60-100 with a telechelic polymer α,ω 12-35, of much lower equivalent grafting ratio $\tau = 0.23\%$. For $C_p = 10\%$ g ml^{-1}, η_{red} of the telechelic sample is 20 and 2 times higher than that of M-12-32-50 and M-12-60-100, respectively. The presence of hydrophobes at the chain ends favours inter-molecular association and then enhances viscosity with respect to a location along the chain. However, comb-like samples have higher molecular weight than telechelic ones. The same observation can be made in Fig. 12b, where M-16-74-100, M-16-32-50 and α,ω-PEOM 16-35 are compared.
- *Distribution of the hydrophobes along the chains.* Fig. 13 shows the strong effect of the distribution of the hydrophobes. Indeed, for a lower average grafting ratio, sample D-08-40-100 solutions are more viscous than those of M-08-60-100.

4. Discussion

These experimental results show that grafted or comb-like samples behave very differently from α–ω telechelic ones, when compared at the same average grafting ratio.

The main differences are:

- a higher solubility characterised by a lower discrepancy of LCST with respect to that of the parent PEO, at least for $\tau < 0.7\%$;
- lower values of CAC, measured by fluorescence but a much broader range where I_1/I_3 values change from the value characteristic of an aqueous environment to that corresponding to a non-polar environment;
- no significant increase of the $\bar{M}_w$ in the case of grafted polymers, up to values of 100 times higher than CAC, while the changes of I_1/I_3 in fluorescence is accompanied by an increase of $\bar{M}_w$ in the case of telechelic ones;
- a much lower viscosity of the comb-like polymers.

Our general interpretation of the behaviour of these two types of sample is schematised in Fig. 1. In the case of telechelic samples, it is now well established that at very low concentration, polymer molecules are isolated, equilibrium existing between loop and extended shapes. At a given critical concentration CAC, flower-like micelles are formed, and in some cases it is possible to interpret the abrupt increase of apparent molecular weight with a model of closed association [22,23]. CAC values obtained by light scattering and fluorescence are similar. When flowers overlap (at $C_p = C_f$), $\bar{M}_w$ decreases again, owing to a strong repulsion between flower PEO corona, and solution viscosity abruptly jumps. This step is generally attributed to formation of inter-"flower" bridges. Simultaneously, the repulsive forces between "flowers" tend to organise them in a cubic array, as well demonstrated in X-rays and neutron-scattering experiments [15,16]. As predicted by Semenov et al. [40], for $C_p > C_f$, viscosimetric and rheological behaviours are no more interpreted in terms of bridges, but are considered to be dominated by osmotic effects.

The scheme we propose for grafted polymers is quite different. We assume that even at very low concentration, $C_p \ll$ CAC, intra-molecular micelles are formed. At a given concentration, corresponding to the overlap of these micelles, which can be called "intra-flowers" (C_f), inter-molecular bridges are formed, which leads to an increase of viscosity. Nevertheless, for $C_p < C_f$, viscosity is expected to be lower than that of the parent polymers, a phenomenon observed in our experiments. Besides, C_f or C_η values must be much higher than the critical overlap concentration of parent PEO, C^*. Table 4 shows that indeed C_η is generally three times higher than C^*. For $C_p \gg C_\eta$, up to now, we do not have much data on the structure of

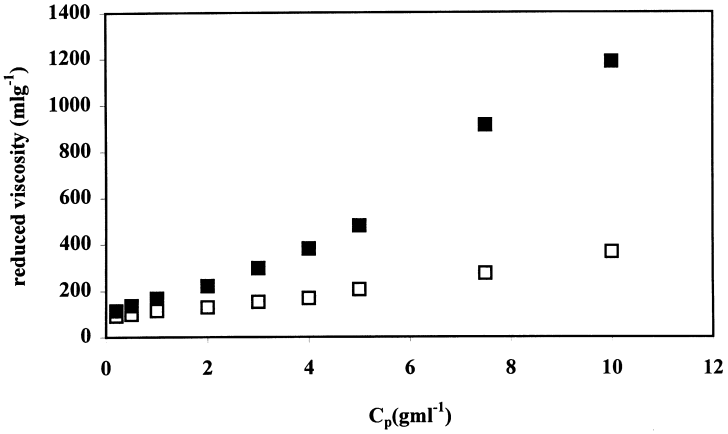

Fig. 13. Reduced viscosity versus concentration, M-08-64-100 (□), and D-08-40-100 (■).

copolymer solutions. However, Fig. 14 shows preliminary neutron-scattering results, which indicate the presence of a broad peak in the scattering curve indicating a liquid order, but less pronounced than that generally observed with telechelics.

In order to verify the validity of this model, we have adjusted our experimental variations of I_1/I_3 by a partition model. Indeed, as already discussed by Anthony et al. [42], the decrease of I_1/I_3 will be completely different if a closed association of hydrophobes occurs at a given CAC (case of the low molecular weight surfactants) or if intra-molecular micelles are already present at $C_p \approx 0$. In the second case, one can calculate I_1/I_3 variations as a function of C_p from a partition coefficient of the probe (pyrene) between water and micelles.

$$K_p = \frac{C_{py}^m}{C_{py}^w} \tag{7}$$

where C_{py}^w and C_{py}^m are the pyrene concentration in water and micelles, respectively, which are taken as two different phases. Then, I_1/I_3 may be considered as the mean of the I_1/I_3 values in each phase.

$$\frac{I_1}{I_3} = \left[\frac{I_1}{I_3}\right]_m + \left[\left(\frac{I_1}{I_3}\right) - \left(\frac{I_1}{I_3}\right)_m\right] \frac{1}{1 + K_p V_{alkyl} C_{alkyl}} \tag{8}$$

C_{alkyl} and V_{alkyl} are the concentration and molar volume of the alkyl chains, respectively.

Fig. 15 gives some examples where the experimental decrease of I_1/I_3 can be very well adjusted by expression (8). This is consistent with our model and with the differences described between telechelic and comb-like systems. As discussed from a theoretical point of view in several papers, the probability of loop formation will depend not only on the average distance between these groups, but also on the fact that they are located along a chain or at its extremities. It can be shown that this probability is higher

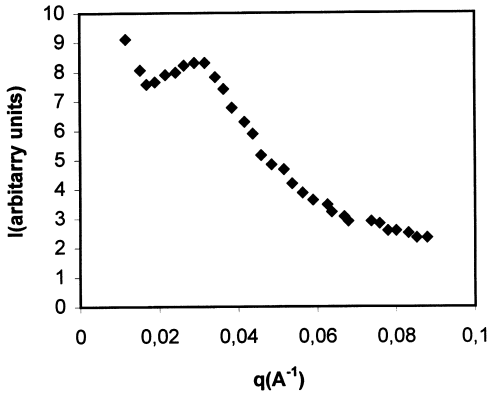

Fig. 14. Neutron scattering curve for sample for M-16-25-50 at 5%.

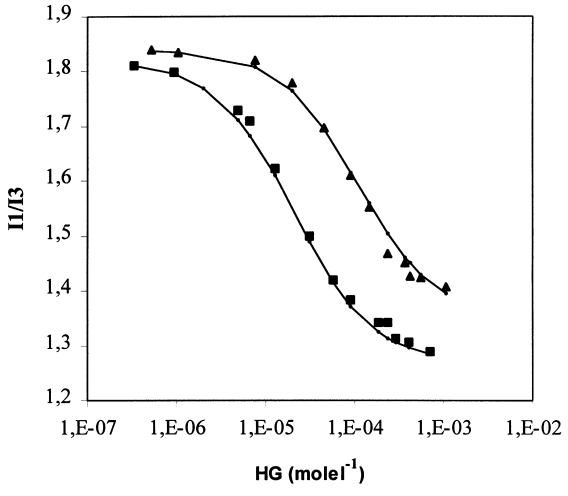

Fig. 15. Adjustments of fluorescence curves with expression (8) sample M-12-45-50 (▲), and sample M-22-30-50 (■).

in the first case and they explain well that inter-molecular association can be favoured for telechelic polymers.

The distribution of the hydrophobic groups along the chain has important effects since the sequentiality tends to favour both inter- and intra-molecular association. At low concentration, the objects will be denser, but above their overlap concentration, the inter-molecular associations are stronger and viscosity increases. Nevertheless, complete theories able to account well for such effects, which have been observed for the associative polymers of comb-like architecture, remains to be developed.

5. Conclusions

The synthesis of a series of comb-like hydrophobically modified PEO and the physico-chemical studies of their association in aqueous solution have allowed us to demonstrate the influence of polymer architecture on the hydrophobic interactions. We conclude that a comb-like architecture favours intra-molecular association with respect to the inter-molecular ones, which leads to aqueous solutions of much lower viscosity than these of telechelic polymers. On the other hand, we confirm that for comb-like polymers, sequentiality of the hydrophobe distribution plays an important role.

References

[1] Glass JE. Polymers in aqueous media, performances through association, Advances in chemistry series, vol. 223. Washington, DC: American Chemical Society, 1989.
[2] Bock J, Siano DB, Schulz DN, Turner SR, Valint Jr. PL, Pace SJ. Proc ACS Div Polym Sci Engng 1986;55:355.
[3] Bock J, Valint Jr. PL, Pace SJ, Siano DB, Schulz DN. In: Schulz DN, editor. Water soluble polymers for petroleum recovery, vol. 147. New York: Plenum Press, 1986.
[4] Schulz DN, Glass JE. Polymers as rheology modifiers, Advances in chemistry series, vol. 462. Washington, DC: American Chemical Society, 1991.
[5] Valint Jr. PL, Bock J, Schulz DN. Polymer in aqueous media, performance through association. Washington, DC: American Chemical Society, 1989 (p. 399).
[6] Bock J, Siano DB, Valint Jr. PL, Pace SJ. Polymers in aqueous media, performance through association. Washington, DC: American Chemical Society, 1989 (p. 411).
[7] Hill A, Candau F, Selb J. Prog Colloid Polym Sci 1991;84:61.
[8] Wang KT, Ilipoulos I, Audebert R. Polym Bull 1988;20:577.
[9] Shalaby SW, McCormick CL, Buttler GB, editors. Water-soluble polymers, synthesis, solution properties and applications ACS symposium series, vol. 467. Washington, DC: American Chemical Society, 1991. p. 218 (chap. 14).
[10] Hill A, Candau F, Selb J. Macromolecules 1993;26:4521.
[11] Biggs S, Hill A, Selb J, Candau F. J Phys Chem 1992;96:1505.
[12] Karusena A, Glass E. Prog Org Coating 1989;17:301.
[13] Persson K, Abrahmsen S, Stilbs P, Hansen FK, Walderhaug H. Colloid Polym Sci 1992;270:465.
[14] Persson K, Wang G, Olofsson G. J Chem Soc Faraday Trans 1994;90:3555.
[15] François J, Alami E, Sarazin D, Maître S, Rawiso M. Colloids Surf 1996;112:251.
[16] Alami E, Rawiso M, Sarazin D, Beinert G, Binana-Limbele W, François J. Hydrophobe polymers, performance with environmental acceptability, Advances in chemistry series, vol. 248. Washington, DC: American Chemical Society, 1995 (chap. 18).
[17] Annable T, Buscall R, Ettelaie R, Whilestone D. J Rheol 1993;37:695.
[18] Annable T, Buscall R, Ettelaie R, Shepherd P, Whilestone D. Langmuir 1994;10:1060.
[19] Jenkins RD. PhD thesis, Lehigh University, Bethlehem, PA, 1990.
[20] Nyström B, Walderhang A, Hansen FK. J Phys Chem 1993;97:7743.
[21] Alami E, Almgren M, Brown W, François J. Macromolecules 1996;29:2229.
[22] Chassenieux C, NicolaÏ T, Durand D. Macromolecules 1997;30:4952.
[23] Gourier C, Maitre S, Sarazin D, Duval M, Beaudoin E, François J. Colloid Interface Sci 2000 (in press).
[24] Abrahmsen-Alami S, Stilbs P. J Phys Chem 1994;98:6359.
[25] Abrahmsen-Alami S, Person K, Stilbs P, Alami E. J Phys Chem 1996;100:4598.
[26] Selb J, Biggs S, Renoux D, Candau F. Hydrophilic polymers, performance with environmental acceptability, Advances in chemistry series, vol. 248. 1995 (p. 251).
[27] Kaezmarski JP, Glass JE. Macromolecules 1993;26:5149.
[28] Fommum G. PhD dissertation, Institute of Organic Chemistry, Norway Technical University, Trondheim, Norway, 1989.
[29] Maitre S. PhD dissertation, Louis Pasteur University, Strasbourg, 1997.
[30] Mouzin G, Cousse H, Rieu JP, Duflos A. Synth Commun 1993;February:117.
[31] Vandenberg EJ. US patent 3135705, 1959.
[32] Vandenberg EJ. US patent 3219591, 1965.
[33] Zana R. In: Zana R, editor. Surfactants solutions. New methods of investigation. New York: Marcel Dekker, 1986.
[34] Chu DY, Thomas JK. In: Rabek JF, editor. Photochemistry and photophysics, vol. 3. Boca Raton, FL: CRC, 1991. p. 49.
[35] Bailey FE, Koliske JV. Alkyline oxide and their polymers. New York/Basel: Marcel Dekker, 1991.
[36] Saeki S, Kuwahara N, Nakata M, Kaneko M. Polymer 1976;17:685.
[37] Kjellander R, Florin E. J Chem Soc Faraday Trans 1981;1(77):2053.
[38] Matsuyama A, Tanaka F. Phys Rev Lett 1990;65(3):341.
[39] Karlström G. J Phys Chem 1985;89:4962.
[40] Semenov AN, Joanny JF, Khoklov AR. Macromolecules 1995;28:1066.
[41] Denavand K, Selser JC. Nature 1990;343:739.
[42] Anthony O, Zana R. Macromolecules 1990;23:2731.